Observation of $e^+e^- \rightarrow K^+K^- J/\psi$ via initial-state radiation at Belle

C. Z. Yuan,[9] C. P. Shen,[9] P. Wang,[9] X. L. Wang,[9] I. Adachi,[7] H. Aihara,[42] K. Arinstein,[1] V. Aulchenko,[1] T. Aushev,[12,17] A. M. Bakich,[37] V. Balagura,[12] E. Barberio,[20] K. Belous,[11] U. Bitenc,[13] A. Bondar,[1] M. Bračko,[13,19] J. Brodzicka,[7] T. E. Browder,[6] Y. Chao,[25] A. Chen,[23] W. T. Chen,[23] B. G. Cheon,[5] R. Chistov,[12] I.-S. Cho,[47] Y. Choi,[36] J. Dalseno,[20] M. Danilov,[12] A. Das,[38] M. Dash,[46] S. Eidelman,[1] D. Epifanov,[1] N. Gabyshev,[1] B. Golob,[13,18] H. Ha,[15] J. Haba,[7] K. Hayasaka,[21] M. Hazumi,[7] D. Heffernan,[31] T. Hokuue,[21] Y. Hoshi,[40] W.-S. Hou,[25] H. J. Hyun,[16] K. Inami,[21] A. Ishikawa,[33] H. Ishino,[43] R. Itoh,[7] Y. Iwasaki,[7] D. H. Kah,[16] J. H. Kang,[47] H. Kawai,[2] T. Kawasaki,[28] H. Kichimi,[7] Y. J. Kim,[4] K. Kinoshita,[3] S. Korpar,[13,19] P. Križan,[13,18] P. Krokovny,[7] R. Kumar,[32] C. C. Kuo,[23] A. Kuzmin,[1] Y.-J. Kwon,[47] M. J. Lee,[35] S. E. Lee,[35] T. Lesiak,[26] S.-W. Lin,[25] D. Liventsev,[12] F. Mandl,[10] A. Matyja,[26] S. McOnie,[37] T. Medvedeva,[12] W. Mitaroff,[10] K. Miyabayashi,[22] H. Miyake,[31] H. Miyata,[28] Y. Miyazaki,[21] R. Mizuk,[12] D. Mohapatra,[46] G. R. Moloney,[20] Y. Nagasaka,[8] M. Nakao,[7] S. Nishida,[7] O. Nitoh,[45] S. Noguchi,[22] T. Nozaki,[7] S. Ogawa,[39] T. Ohshima,[21] S. Okuno,[14] S. L. Olsen,[6,9] P. Pakhlov,[12] G. Pakhlova,[12] C. W. Park,[36] H. Park,[16] L. S. Peak,[37] L. E. Piilonen,[46] H. Sahoo,[6] Y. Sakai,[7] O. Schneider,[17] J. Schümann,[7] K. Senyo,[21] M. E. Sevior,[20] M. Shapkin,[11] H. Shibuya,[39] J.-G. Shiu,[25] B. Shwartz,[1] J. B. Singh,[32] A. Somov,[3] S. Stanič,[29] M. Starič,[13] T. Sumiyoshi,[44] F. Takasaki,[7] K. Tamai,[7] M. Tanaka,[7] Y. Teramoto,[30] I. Tikhomirov,[12] S. Uehara,[7] T. Uglov,[12] Y. Unno,[5] S. Uno,[7] P. Urquijo,[20] Y. Usov,[1] G. Varner,[6] K. Vervink,[17] S. Villa,[17] C. C. Wang,[25] C. H. Wang,[24] Y. Watanabe,[14] E. Won,[15] B. D. Yabsley,[37] A. Yamaguchi,[41] Y. Yamashita,[27] M. Yamauchi,[7] C. C. Zhang,[9] Z. P. Zhang,[34] A. Zupanc,[13] and O. Zyukova[1]

(Belle Collaboration)

[1]*Budker Institute of Nuclear Physics, Novosibirsk*
[2]*Chiba University, Chiba*
[3]*University of Cincinnati, Cincinnati, Ohio 45221*
[4]*The Graduate University for Advanced Studies, Hayama*
[5]*Hanyang University, Seoul*
[6]*University of Hawaii, Honolulu, Hawaii 96822*
[7]*High Energy Accelerator Research Organization (KEK), Tsukuba*
[8]*Hiroshima Institute of Technology, Hiroshima*
[9]*Institute of High Energy Physics, Chinese Academy of Sciences, Beijing*
[10]*Institute of High Energy Physics, Vienna*
[11]*Institute of High Energy Physics, Protvino*
[12]*Institute for Theoretical and Experimental Physics, Moscow*
[13]*J. Stefan Institute, Ljubljana*
[14]*Kanagawa University, Yokohama*
[15]*Korea University, Seoul*
[16]*Kyungpook National University, Taegu*
[17]*École Polytechnique Fédérale de Lausanne (EPFL), Lausanne*
[18]*University of Ljubljana, Ljubljana*
[19]*University of Maribor, Maribor*
[20]*University of Melbourne, School of Physics, Victoria 3010*
[21]*Nagoya University, Nagoya*
[22]*Nara Women's University, Nara*
[23]*National Central University, Chung-li*
[24]*National United University, Miao Li*
[25]*Department of Physics, National Taiwan University, Taipei*
[26]*H. Niewodniczanski Institute of Nuclear Physics, Krakow*
[27]*Nippon Dental University, Niigata*
[28]*Niigata University, Niigata*
[29]*University of Nova Gorica, Nova Gorica*
[30]*Osaka City University, Osaka*
[31]*Osaka University, Osaka*
[32]*Panjab University, Chandigarh*
[33]*Saga University, Saga*
[34]*University of Science and Technology of China, Hefei*
[35]*Seoul National University, Seoul*
[36]*Sungkyunkwan University, Suwon*

^{37}*University of Sydney, Sydney, New South Wales*
^{38}*Tata Institute of Fundamental Research, Mumbai*
^{39}*Toho University, Funabashi*
^{40}*Tohoku Gakuin University, Tagajo*
^{41}*Tohoku University, Sendai*
^{42}*Department of Physics, University of Tokyo, Tokyo*
^{43}*Tokyo Institute of Technology, Tokyo*
^{44}*Tokyo Metropolitan University, Tokyo*
^{45}*Tokyo University of Agriculture and Technology, Tokyo*
^{46}*Virginia Polytechnic Institute and State University, Blacksburg, Virginia 24061*
^{47}*Yonsei University, Seoul*

The process $e^+e^- \to K^+K^-J/\psi$ is observed for the first time via initial-state radiation. The cross section of $e^+e^- \to K^+K^-J/\psi$ for center-of-mass energies between threshold and 6.0 GeV is measured using 673 fb^{-1} of data collected with the Belle detector on and off the $\Upsilon(4S)$ resonance. No significant signal for $Y(4260) \to K^+K^-J/\psi$ is observed, and we determine $\mathcal{B}(Y(4260) \to K^+K^-J/\psi)\Gamma(Y(4260) \to e^+e^-) < 1.2$ eV/c^2 at a 90% confidence level. We also find evidence for $e^+e^- \to K^0_S K^0_S J/\psi$ in the same data sample.

The study of charmonium states via initial-state radiation (ISR) at the *B*-factories has proven to be very fruitful. In the process $e^+e^- \to \gamma_{\mathrm{ISR}}\pi^+\pi^-J/\psi$, the *BABAR* Collaboration observed the $Y(4260)$ [1]. This structure was also observed by the CLEO [2] and Belle Collaborations [3] with the same technique; moreover, there is a broad structure near 4.05 GeV/c^2 in the Belle data. In a subsequent search for the $Y(4260)$ in the $e^+e^- \to \gamma_{\mathrm{ISR}}\pi^+\pi^-\psi(2S)$ process, *BABAR* found a structure at around 4.32 GeV/c^2 [4], while the Belle Collaboration observed two resonant structures at 4.36 GeV/c^2 and 4.66 GeV/c^2 [5]. Recently, CLEO collected 13.2 pb^{-1} of data at $\sqrt{s} = 4.26$ GeV and investigated 16 decay modes with charmonium or light hadrons [6]. The large $e^+e^- \to \pi^+\pi^-J/\psi$ cross section at this energy is confirmed. In addition, there is also evidence for K^+K^-J/ψ (3.7σ) based on three events observed. Further investigation on the process $e^+e^- \to K^+K^-J/\psi$ will shed light on the understanding of the $Y(4260)$ and the other vector charmonium states.

In this paper, we use a 673 fb^{-1} data sample collected near the $\Upsilon(4S)$ with the Belle detector [7] operating at the KEKB asymmetric-energy e^+e^- (3.5 on 8 GeV) collider [8] to investigate the K^+K^-J/ψ final state produced via ISR. About 90% of the data were collected at the $\Upsilon(4S)$ resonance ($\sqrt{s} = 10.58$ GeV), and the rest were taken at a center-of-mass (CM) energy that is 60 MeV below the $\Upsilon(4S)$ peak.

We use PHOKHARA [9] that was validated in a previous analysis [3] to generate signal events. In the generator, one or two photons are allowed to be emitted before forming the resonance *X*, then *X* decays into K^+K^-J/ψ with J/ψ decays into e^+e^- or $\mu^+\mu^-$. When generating the Monte Carlo (MC) sample, the mass of the *X* is fixed to a certain value while the width is set to zero. In $X \to K^+K^-J/\psi$, a pure *S*-wave between the K^+K^- system

and the J/ψ, as well as between the K^+ and K^- is assumed. The invariant mass of the K^+K^- system is generated according to phase space. To estimate the model uncertainty, we also generate events with K^+K^- invariant mass distributed like $m_{\pi^+\pi^-}$ in $\psi(2S) \to \pi^+\pi^-J/\psi$ decays [10], i.e., $\frac{d\sigma}{dm_{K^+K^-}} \propto$ phase space $\times (m^2_{K^+K^-} - 4m^2_K)^2$.

We select candidate events with criteria similar to those used for the analysis of $e^+e^- \to \pi^+\pi^-J/\psi$ [3]. We require the number of charged tracks to be four with a zero net charge. For these tracks, the impact parameters perpendicular to and along the beam direction with respect to the interaction point are required to be less than 0.5 and 4 cm, respectively, and the transverse momentum is restricted to be higher than 0.1 GeV/c. For each charged track, information from different detector subsystems is combined to form a likelihood for each particle species (i), $\mathcal{L}_i$ [11]. Tracks with $\mathcal{R}_K = \frac{\mathcal{L}_K}{\mathcal{L}_K + \mathcal{L}_\pi} > 0.6$ are identified as kaons with an efficiency of about 92% for the tracks of interest; about 4% are misidentified π tracks [11]. Similar likelihood ratios are formed for electron and muon identification. For electrons from $J/\psi \to e^+e^-$, one track should have $\mathcal{R}_e > 0.95$ while the other track has $\mathcal{R}_e > 0.05$, this results in a very pure $J/\psi \to e^+e^-$ sample with an efficiency of 90%; for muons from $J/\psi \to \mu^+\mu^-$, at least one track is required to have $\mathcal{R}_\mu > 0.95$; in cases where one of the tracks has no muon identification (ID) information, the polar angles of the two muon tracks in the $K^+K^-\mu^+\mu^-$ center-of-mass system are required to satisfy $-0.7 < \cos\theta_\mu < 0.7$ based on a comparison between data and MC simulation. The efficiency for $J/\psi \to \mu^+\mu^-$ is 87%. Events with γ-conversions are removed by requiring $\mathcal{R}_e < 0.75$ for the K^+K^- tracks. For the $J/\psi \to e^+e^-$ mode, γ-conversion events are further suppressed by requiring a K^+K^- invariant mass greater than 1.05 GeV/c^2; this also removes events with a ϕ signal in the final state.

For the $J/\psi \to \mu^+\mu^-$ mode, we require a K^+K^- invariant mass outside a ± 10 MeV/c^2 interval around the ϕ mass to remove events with a ϕ signal in the final state, possibly produced via $e^+e^- \to \gamma\gamma^*\gamma^* \to \gamma\phi\ell^+\ell^-$. The detection of the ISR photon is not required, instead, we identify ISR events by the requirement $|M_{rec}^2| < 1.0$ (GeV/c^2)^2, where M_{rec}^2 is the square of the mass that is recoiling from the four charged tracks. The M_{rec}^2 requirement is tighter than that in our previous analyses [3,5] as the M_{rec}^2 resolution has improved, due to the lower momenta of the particles in K^+K^-J/ψ as compared to the $\pi^+\pi^-J/\psi$ and $\pi^+\pi^-\psi(2S)$ final states.

Clear J/ψ signals are observed in both decay modes. We define a J/ψ signal region as 3.06 GeV/$c^2 < m_{\ell^+\ell^-} <$ 3.14 GeV/c^2 (the bremsstrahlung photons in the e^+e^- final state are included, and the mass resolution is about 17 MeV/c^2), and J/ψ mass sidebands as 2.91 GeV/$c^2 <$ $m_{\ell^+\ell^-} <$ 3.03 GeV/c^2　　or　　3.17 GeV/$c^2 < m_{\ell^+\ell^-} <$ 3.29 GeV/c^2; the latter are 3 times as wide as the signal region.

Figure 1 shows the K^+K^-J/ψ invariant mass [12] distribution after the above selection, together with the background estimated from the J/ψ mass sidebands. There is a broad enhancement around 4.4–5.5 GeV/c^2. In addition, there are two events near $\sqrt{s} = 4.26$ GeV, where CLEO observes three K^+K^-J/ψ events [6]. It is evident from the figure that the background estimated from the J/ψ sidebands is low, which indicates that the background from non-J/ψ final states is small. The backgrounds not measured from the sidebands, such as XJ/ψ, with X not being K^+K^-, are found from MC simulation to be less than one event and are neglected.

The data points in Figs. 2(a) and 2(b) show the M_{rec}^2 distribution (the requirement on it has been relaxed) and the polar angle distribution of the K^+K^-J/ψ system in the e^+e^- CM frame for the selected K^+K^-J/ψ events with invariant mass between 4.4 and 5.2 GeV/c^2. The data

FIG. 2 (color online). M_{rec}^2 distribution (a) and the polar angle distribution of the K^+K^-J/ψ system in the e^+e^- CM frame (b) for the selected K^+K^-J/ψ events with invariant masses between 4.4 and 5.2 GeV/c^2. The points with error bars are data, the shaded histograms are the normalized J/ψ sideband distributions, and the solid histograms are MC simulated events, normalized to the measured cross section and integrated luminosity. The background from J/ψ mass sidebands has been added to the MC simulation.

agree well with the MC simulation (shown as open histograms), indicating the existence of signals that are produced from ISR.

We estimate the significance of the events between threshold and 6.0 GeV/c^2 by calculating the probability that the estimated number of background events in the normalized J/ψ sidebands (12.3 ± 2.0) fluctuates to the number of observed events in the J/ψ signal region (93) or more. It is found that the above probability is very small, corresponding to a statistical significance for the signal much larger than 10σ.

The $e^+e^- \to K^+K^-J/\psi$ cross section for each K^+K^-J/ψ mass bin is computed with

$$\sigma_i = \frac{n_i^{obs} - n_i^{bkg}}{\varepsilon_i \mathcal{L}_i \mathcal{B}(J/\psi \to \ell^+\ell^-)}, \qquad (1)$$

where n_i^{obs}, n_i^{bkg}, ε_i, and $\mathcal{L}_i$ are the number of events observed in data, the number of background events from a fit to the J/ψ sideband events, the efficiency, and the effective luminosity [13] in the ith K^+K^-J/ψ mass bin, respectively [14]. Because of the low statistics, we fit the background distribution with a second-order polynomial and take the fit number as the background in each K^+K^-J/ψ mass bin. The dilepton branching fraction, $\mathcal{B}(J/\psi \to \ell^+\ell^-) = 11.87\%$, is taken from Ref. [15]. The resulting cross sections are shown in Fig. 3, where the error bars indicate the combined statistical errors of the signal and the background events [16]. The cross section we measure in the 4.25–4.30 GeV bin is consistent with the direct measurement at $\sqrt{s} = 4.26$ GeV by the CLEO experiment [6].

There are a few sources of systematic errors for the cross section measurement. The particle ID uncertainty, measured using the same method as in Ref. [3] with pure track samples, is 4%; the uncertainty in the tracking efficiency
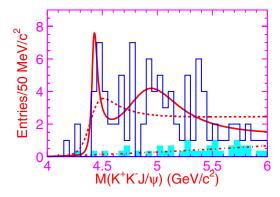

FIG. 1 (color online). The K^+K^-J/ψ invariant mass distribution. The open histogram is the selected data while the shaded histogram shows the normalized sideband events. The solid (dashed) curve shows the best fit with two (one) Breit-Wigner functions and an incoherent background term, while the dash-dotted curve indicates a fit to the sideband background.
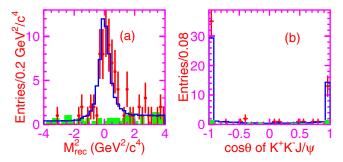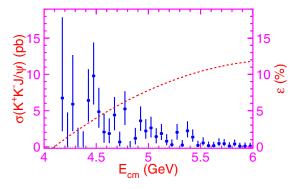
FIG. 3 (color online). The measured $e^+e^- \to K^+K^-J/\psi$ cross section for CM energies between threshold and 6.0 GeV (points with error bars). The errors are statistical only; a 10% systematic error that is common to all the data points is not included. Bins without points have a central value of zero. The dashed curve shows the energy-dependent selection efficiency with scale in the right-hand side.

for tracks with angles and momenta characteristic of signal events is about 1%/track, and is additive; efficiency uncertainties associated with the J/ψ mass and M_{rec}^2 requirements are also determined from a study of the very pure $e^+e^- \to \psi(2S) \to \pi^+\pi^-J/\psi$ event sample. In this study we find that the detection efficiency is lower than that inferred from the MC simulation by $(2.5 \pm 0.4)\%$ relatively. A correction factor is applied to the final results and 0.4% is included in the systematic error. Belle measures the luminosity with a precision of 1.4%, and the uncertainty of the ISR photon radiator is 0.1% [13]. The main uncertainty in the PHOKHARA generator [9] is due to the modelling of the K^+K^- mass spectrum. Figure 4 shows the K^+K^- invariant mass versus K^+K^-J/ψ invariant mass, as well as the projection on the K^+K^- invariant mass for events in the J/ψ signal region. The K^+K^- invariant mass tends to be large and close to the phase space boundary, with an accumulation of events at 1.2 GeV/c^2 and 1.7 GeV/c^2. Simulations with modified K^+K^- invariant mass distributions yield efficiencies that are higher by 2%–5% for different K^+K^-J/ψ masses.

TABLE I. Systematic errors of the cross section measurement. They are common for all data points.

Source	Relative error (%)
Particle ID	4
Tracking efficiency	4
J/ψ mass and M_{rec}^2 selection	0.4
Integrated luminosity	1.4
$m_{K^+K^-}$ distribution	5
Background estimation	6
Trigger efficiency	1
Branching fractions	1
MC statistics	1.5
Sum in quadrature	10

This is not corrected for in the analysis, but is taken as the systematic error (conservatively estimated as 5%) for all K^+K^-J/ψ mass values. The angular distributions of the final state particles are compared with the MC generation; no evidence was found for non-S-wave components. Estimating the backgrounds using different J/ψ mass sidebands results in a change of background events at the 0.18/50 MeV/c^2 level, corresponding to an average of about a 6% change in the cross section. According to the MC simulation, the trigger efficiency for the final state is 98%, with an uncertainty that is smaller than 1%. From Ref. [15], the uncertainty on the world averages for $\mathcal{B}(J/\psi \to \ell^+\ell^-) = \mathcal{B}(J/\psi \to e^+e^-) + \mathcal{B}(J/\psi \to \mu^+\mu^-)$, determined by linearly adding the errors for the e^+e^- and $\mu^+\mu^-$ modes, is 1%. Finally, the MC statistical error on the efficiency is 1.5%. These errors are summarized in Table I. Assuming that all the sources are independent and adding them in quadrature, we obtain a total systematic error on the cross section of 10%.

An unbinned maximum likelihood fit is applied to the K^+K^-J/ψ mass spectrum in Fig. 1. Here the theoretical shape is multiplied by the efficiency and effective luminosity, which are functions of the K^+K^-J/ψ invariant mass. The Breit-Wigner function for a spin one resonance decaying into final state f with mass (M), total width (Γ_{tot}),
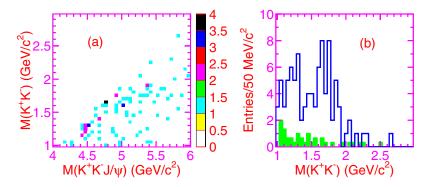

FIG. 4 (color online). Scatter plot of $m_{K^+K^-}$ versus $m_{K^+K^-J/\psi}$ (a) and the projection on the K^+K^- invariant mass (b) for events in the J/ψ signal region. The shaded histogram is the distribution of the normalized sideband events.
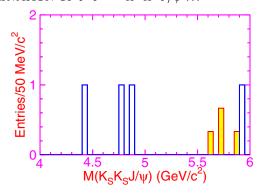
FIG. 5 (color online). $K_S^0 K_S^0 J/\psi$ invariant mass distribution of the selected $e^+e^- \rightarrow K_S^0 K_S^0 J/\psi$ candidates, the blank histogram is for events in the J/ψ signal region, while the shaded histogram is the normalized sideband backgrounds.

and partial width to e^+e^- ($\Gamma_{e^+e^-}$) is

$$\sigma(s) = \frac{M^2}{s} \frac{12\pi\Gamma_{e^+e^-}\mathcal{B}(R \rightarrow f)\Gamma_{\text{tot}}}{(s - M^2)^2 + M^2\Gamma_{\text{tot}}^2} \frac{PS(\sqrt{s})}{PS(M)}, \quad (2)$$

where $\mathcal{B}(R \rightarrow f)$ is the branching fraction of the resonance to final state f, and $PS(\sqrt{s})$ is the three-body decay phase space factor for $X \rightarrow K^+K^-J/\psi$. The MC-determined mass resolution varies from 3 MeV/c^2 at $m_{K^+K^-J/\psi} = 4.3$ GeV/c^2 to 6.8 MeV/c^2 at 5.4 GeV/c^2. This is small compared to the widths of the resonances in our study and is neglected.

We fit the K^+K^-J/ψ invariant mass spectrum with one Breit-Wigner plus a background term. The latter is a second-order polynomial that is fit to the scaled sideband data. The dashed curve in Fig. 1 shows the fit results. The resonance parameters are $M = 4430^{+38}_{-43}$ MeV/c^2, $\Gamma_{\text{tot}} = 254^{+55}_{-46}$ MeV/c^2, $\mathcal{B}(R \rightarrow K^+K^-J/\psi) \cdot \Gamma_{e^+e^-} = 1.9 \pm 0.3$ eV/c^2, where the errors are statistical only. Although the peak mass is close to the $\psi(4415)$, Γ_{tot} is larger than its world average of 62 ± 20 MeV/c^2 [15]. To determine the goodness of fit, we bin the data so that the minimum expected number of events in a bin is at least seven and determine a $\chi^2/ndf = 10.7/6$, corresponding to a confidence level (C.L.) of 10%. Adding a coherent $Y(4260)$ amplitude in the fit with mass and width fixed at the Belle measurement [3] yields an upper limit on $\mathcal{B}(Y(4260) \rightarrow K^+K^-J/\psi)\Gamma(Y(4260) \rightarrow e^+e^-) < 1.2$ eV/c^2 at 90% C.L. A fit using the above functions together with a coherent $\psi(4415)$ component with mass and width fixed at its world average [15] values improves the fit (solid curve in Fig. 1) to $\chi^2/ndf = 4.2/4$, C.L. = 38%; the significance of the $\psi(4415)$ signal is found to be around 1.7σ with a branching fraction for $\psi(4415) \rightarrow$

K^+K^-J/ψ at the few per mille level; in this fit, the mass and width of the second Breit-Wigner become 4875 ± 132 MeV/c^2 and 630 ± 126 MeV/c^2, respectively.

We also search for $e^+e^- \rightarrow K_S^0 K_S^0 J/\psi$ with the same data sample. All the selection criteria are the same as for K^+K^-J/ψ except that the selection of K^+K^- is replaced by the selection of two K_S^0's decaying into $\pi^+\pi^-$ [17]. After selection, the invariant mass distribution of the $K_S^0 K_S^0 J/\psi$ candidates is shown in Fig. 5. Three events (one $J/\psi \rightarrow e^+e^-$ and two $J/\psi \rightarrow \mu^+\mu^-$) are observed between 4.4 and 5.2 GeV/c^2 where a large K^+K^-J/ψ signal is observed. In the higher mass region, the number of events in the J/ψ signal region is about the same as expected from the normalized sideband events.

MC simulation yields an average selection efficiency of $\varepsilon = (0.50 \pm 0.04)\%$ for $m_{K_S^0 K_S^0 J/\psi} \in [4.4, 5.2]$ GeV/c^2. Assuming that there is no background, we obtain the average cross section for $e^+e^- \rightarrow K_S^0 K_S^0 J/\psi$ of $\bar{\sigma}_{K_S^0 K_S^0 J/\psi} = 1.8^{+1.4}_{-1.1}$ pb, where the error is statistical only. The average cross section for $e^+e^- \rightarrow K^+K^-J/\psi$ in the same mass range is $\bar{\sigma}_{K^+K^-J/\psi} = 3.1 \pm 0.6$ pb, where the error includes combined statistical and systematic uncertainties. From the above two cross sections, we obtain $R = \frac{\bar{\sigma}_{K_S^0 K_S^0 J/\psi}}{\bar{\sigma}_{K^+K^-J/\psi}} = 0.6^{+0.5}_{-0.4}$, in agreement with the expectation ($R = 1/2$) from isospin symmetry.

In summary, the process $e^+e^- \rightarrow K^+K^-J/\psi$ is observed and the cross section is measured for the CM energy between threshold and 6.0 GeV. There is one very broad structure; fits using either a single Breit-Wigner function, or a $\psi(4415)$ plus a second Breit-Wigner function yield resonance parameters that are very different from those of the excited ψ states currently listed in Refs. [15,18]. We observe two events near the $Y(4260)$ mass, with a cross section consistent with the CLEO measurement [6] at $\sqrt{s} = 4.26$ GeV within the large errors. We set an upper limit on $\mathcal{B}(Y(4260) \rightarrow K^+K^-J/\psi)\Gamma(Y(4260) \rightarrow e^+e^-) < 1.2$ eV/c^2 at 90% C.L.

[1] B. Aubert *et al.* (*BABAR* Collaboration), Phys. Rev. Lett. **95**, 142001 (2005).
[2] Q. He *et al.* (CLEO Collaboration), Phys. Rev. D **74**, 091104(R) (2006).
[3] C. Z. Yuan *et al.* (Belle Collaboration), Phys. Rev. Lett. **99**, 182004 (2007).
[4] B. Aubert *et al.* (*BABAR* Collaboration), Phys. Rev. Lett. **98**, 212001 (2007).
[5] X. L. Wang *et al.* (Belle Collaboration), Phys. Rev. Lett. **99**, 142002 (2007).
[6] T. E. Coan *et al.* (CLEO Collaboration), Phys. Rev. Lett. **96**, 162003 (2006).
[7] A. Abashian *et al.* (Belle Collaboration), Nucl. Instrum. Methods Phys. Res., Sect. A **479**, 117 (2002).
[8] S. Kurokawa and E. Kikutani, Nucl. Instrum. Methods Phys. Res., Sect. A **499**, 1 (2003), and other papers included in this volume.
[9] G. Rodrigo, H. Czyż, J. H. Kühn, and M. Szopa, Eur. Phys. J. C **24**, 71 (2002).
[10] J. Z. Bai *et al.* (BES Collaboration), Phys. Rev. D **62**, 032002 (2000).
[11] E. Nakano, Nucl. Instrum. Methods Phys. Res., Sect. A **494**, 402 (2002).
[12] In this paper, $m_{K^+K^-\ell^+\ell^-} - m_{\ell^+\ell^-} + m_{J/\psi}$ is used instead of the invariant mass of the four final-state particles to improve the mass resolution. Here $m_{J/\psi}$ is the nominal mass of J/ψ.
[13] E. A. Kuraev and V. S. Fadin, Yad. Fiz. **41**, 733 (1985) [Sov. J. Nucl. Phys. **41**, 466 (1985)].
[14] For the bins with no observed events, the number of background events is taken to be zero when calculating the 68.3% C.L. intervals.
[15] W.-M. Yao *et al.* (Particle Data Group), J. Phys. G **33**, 1 (2006).
[16] J. Conrad *et al.*, Phys. Rev. D **67**, 012002 (2003).
[17] F. Fang, Ph.D thesis, University of Hawaii, 2003.
[18] M. Ablikim *et al.* (BES Collaboration), arXiv:0705.4500.